JCTC Journal of Chemical Theory and Computation

Ab Initio Study of Water Polarization in the Hydration Shell of Aqueous Hydroxide: Comparison between Polarizable and Nonpolarizable Water Models

Denis Bucher,[†] Angus Gray-Weale,[‡] and Serdar Kuyucak*

School of Physics, University of Sydney, NSW 2006, Australia

Received July 1, 2010

Abstract: Ab initio simulations of aqueous hydroxide are performed to study the structure and polarization of water molecules in the first solvation shell. Polarization is found to depend on the configuration of the hydrogen-bond (HB) donors. In the most common case of four HB donors, the dipole moment of water molecules is much larger than those in the first shell of monovalent ions. When there are only three HB donors, the water dipole moment exceeds even those in the first shell of a divalent cation. We also show that the dipole fluctuations in the first hydration shell of hydroxide are reduced compared to bulk water, which can provide a rationale for the propensity of hydroxide for interfaces with hydrophobes. Because of its unique properties, hydroxide provides a nontrivial test for benchmarking classical models. Comparison of the ab initio results with those obtained from the classical models indicates that the latter need to be further improved in order to yield reliable results.

Introduction

Water's autolysis into hydronium (H_3O^+) and hydroxide (OH^-) ions is important because these ions affect and even control many biological and chemical processes. While the fast diffusion of these ions relative to water has been explained via the Grotthus mechanism,[1] involving transfer of a proton along a hydrogen bond (HB), a truly microscopic understanding of this mechanism has only been obtained recently with the application of the ab initio molecular dynamics (AIMD) simulations to aqueous solutions. Proton solvation and transport, in particular, has attracted a great deal of attention and has been studied by both ab initio[2−7] and empirical valence bond models.[8−15] According to the picture emerging from these studies, there is no dominant structure for the hydronium ion, but rather it continuously evolves between the Eigen complex with three HB acceptors, $[H_3O^+ \cdot (H_2O)_3]$ and the Zundel cation, $[H_2O \cdots H \cdots OH_2]$. Proton transfer from the hydronium ion to a neighboring water molecule is facilitated when one of the HB's in the receiving water breaks so that it attains a similar solvation structure to that of hydronium (according to the presolvation concept).[16]

From symmetry arguments, a similar mechanism involving proton holes had been assumed to operate in hydroxide transport.[17,18] In this mirror-image analogy, hydroxide accepts three HB's and donates none, and a proton is transferred from a neighboring water molecule to the hydroxide along the HB. A difficulty with this mechanism is that, while the donor water is tetrahedrally coordinated, the water derived from the hydroxide after the proton transfer is only three-fold coordinated, in conflict with the presolvation concept. Indeed, the pioneering AIMD simulations of aqueous hydroxide indicated that the situation is much more complex than that suggested by the mirror mechanism.[2,16,19,20] The dominant solvation configuration is hypercoordinated with four HB donors, and the three-fold coordination occurs intermittently as a result of fluctuations. Also the hydroxide hydrogen is a HB donor most of the time. The difficulty of obtaining the right solvation structure for hydroxide was highlighted when another AIMD simulation of hydroxide using a different density functional (PW91[21] instead of BLYP)[22,23] found the three-fold coordination as the dominant

* Corresponding author. E-mail: serdar@physics.usyd.edu.au. Telephone: (61) 2 9036 5306.

[†] Present address: Department of Chemistry and Biochemistry, University of California, San Diego, La Jolla, CA 92093-0365.

[‡] Present address: School of Chemistry, Monash University, Clayton 3800, Victoria, Australia.

10.1021/ct1003719
Published on Web 08/19/2010

structure.[24] Further investigation of this issue including a third density functional (HCTH)[25] confirmed the previous solvation structures obtained with BLYP and PW91 and further showed that use of the HCTH functional led to a further stabilization of the configuration with four HB donors.[26] The question of which functional to use was settled by looking at the dynamics—PW91 led to an ultrafast diffusion of hydroxide, while that of HCTH was too slow, and only BLYP gave a diffusion coefficient in reasonable agreement with the experimental data.[26,27] This suggests that the solvation structure obtained using BLYP is the most realistic one. This structure is also supported by the neutron diffraction[28,29] and solution X-ray diffraction experiments,[30] which are consistent with four strongly bound HB donors and a more weakly bound HB acceptor.

A recent debate about the surface affinity of hydronium and hydroxide ions has accentuated the need for accurate modeling of these ions. From oil droplet and air bubble experiments,[31,32] it has long been known that the surface of neat water is negatively charged, indicating that hydroxide has a higher affinity for a hydrophobic surface than hydronium. In contrast, recent spectroscopic experiments based on second harmonic generation have found that hydronium is enhanced at the surface, while hydroxide is not.[33,34] More recent spectroscopic work did detect a strong hydroxide adsorption at an octadecyltrichlorosilane—water interface,[35] in agreement with predictions of electrokinetic and stoichiometric experiments which show very similar charges at oil—water and air—water interfaces across several pH units.[36] We note that the sum frequency and the second harmonic generation experiments probe mainly the top layer of water molecules at the surface, while the macroscopic electrokinetic experiments probe the charge inside the shear plane, within about 2.5 nm of the interface, so the two sets of experiments do not necessarily contradict each other. An explanation for these observations has recently been published that depends on the hydroxide's constraint of neighboring water molecules. An accurate description of this effect is needed to explore further the hydroxide's surface affinity.[37]

Whether the water surface is acidic or basic is important in atmospheric chemical processes, such as absorption of carbon dioxide at the ocean surface.[38] Therefore this issue has prompted many computational investigations of the surface affinity of hydronium and hydroxide ions. As in the case of solvation structure, hydronium has attracted more attention, and its surface affinity has been studied using classical MD,[39−41] empirical models,[42,43] and AIMD.[44,46] There is a broad agreement among these studies that hydronium weakly binds to the interfacial region behaving like an amphiphilic molecule. The calculated free energy minimum is about 1−2 kcal/mol in all three approaches, e.g., 0.7 in polarizable MD,[41] 1.8 kcal/mol in the empirical valence bond model,[43] and 1.3 in AIMD.[46] The situation for hydroxide is less clear. Classical MD results find a slight repulsion of hydroxide from the interface,[40] the empirical model predicts a completely flat free energy profile for hydroxide,[47] while AIMD simulations indicate that it is attracted to the surface.[44,45] The diversity of results is perhaps not surprising when one considers that even within the AIMD simulations the solvation structure of hydroxide is quite sensitive to the chosen density functional and that several approximations are often made in practice, such as the neglect of nuclear quantum effects or the absence of counterions. Furthermore, the conditions of an AIMD simulation are very different from those of a typical experiment. For instance, the concentration of hydroxide is very high, and both the sampling and size of the system are rather limited. Nevertheless AIMD has been shown to provide an accurate description of the solvation shell of ions, and in that regard, it can be used to help improve modeling of hydroxide and resolve the differences among various empirical approaches.

Here we perform AIMD simulations of aqueous hydroxide to study the structure and polarization of the solvation waters. AIMD simulations have been previously used to study the polarization of solvation waters for various ionic systems[48−55] but not for hydroxide. Because of its unique properties, aqueous hydroxide provides a thorough benchmark for classical models. By the same token, the polarization properties of solvation waters obtained from the AIMD simulations could provide useful insights in the development of polarizable water models. The paper is organized as follows: First, we compare the AIMD simulation results of hydroxide in water with those of classical simulations. Second, we analyze the different coordination geometries that coexist in the first hydration shell in AIMD simulations and report the dipole of waters in the first hydration shell. Finally, we consider the dipole fluctuations around the hydroxide and show that they are significantly reduced compared to bulk water.

Methods

Classical Simulations. We studied three classical models for the solvation of the hydroxide ion. The first two are based on TIP3P[56] and SPC/E[57] water models, which are rigid and nonpolarizable. They use the same hydroxide model, with a bond length of 1 Å and a charge on the hydrogen of +0.41e. We examined also hydroxide models with larger and smaller dipole moments, but these led to no essential difference in our conclusions. The third model includes electronic polarizability for all species and was recently described in ref 58. It is based on the POL3 water model. All the classical simulations were done with the NVT ensemble at the experimental density, and the temperature was controlled using the Langevin method or a Nose—Hoover chain thermostat.[59−61] A counterion was included to neutralize the hydroxide system.

TIP3P and SPC/E Simulations. Simulations of the nonpolarizable models were done using the program NAMD.[62] Simulations of 512 water molecules at the experimental density were equilibrated initially for 10 ps at 298 K. The end point of this run was used to generate 25 starting configurations with the same positions but different velocities. These 25 configurations were equilibrated for 100 ps and then run for a further 100 ps to collect data on the structure and dielectric fluctuations. Note that this equilibration time is roughly 10 times the dielectric relaxation time

of about 10 ps. The same procedure was followed for models with 511 water molecules and a single hydroxide in the same volume, except that data were collected for 500 ps after equilibration for 100 ps. In all these simulations, the time step was 1 fs, all bonds were held rigid, and the cutoff for nonbonded interactions was 9 Å. The long-range electrostatic interactions were handled using the particle mesh Ewald (PME) method[63] based on a grid of 24^3 points.

POL3 Simulations. Simulations of the polarizable model were done with the toyMD program.[64] The hydroxide model is described in ref 58. It is based on an optimized fixed point charge model for hydroxide, parametrized with MP2 calculations, and used with the polarizable water model (POL3).[65] A simulation of 512 water molecules at the experimental density was split into 25 runs with different initial velocities, each was equilibrated for 20 ps, and the radial distribution functions (RDFs) and fluctuation data were then collected from each system over 40 ps. We verified with the nonpolarizable models that this much shorter simulation time is adequate for pure water, in part because we can calculate the fluctuation distributions by averaging over each molecule in the simulation. We studied also a single hydroxide with 510 POL3 waters in the same box. This system was equilibrated for 20 ps and then split into 25 runs, starting from the same positions but different velocities. Each of these 25 was equilibrated for 20 ps, and then data were collected during a further 40 ps, to give a total of 1 ns. Again, we confirmed by examining the rigid models that these equilibration times are ample. All polarizable runs used a time step of 1.25 fs, constrained the bonds to be of fixed length with the SHAKE algorithm,[66] used a cutoff for nonbonded interactions of 10.6 Å, and used the P^3M method[67] on a grid of 18^3 points. Induced dipoles were calculated by a simple iterative procedure at each time step.

Ab initio Simulations. The initial coordinates for the quantum mechanics (QM) simulations were taken from equilibrated structures obtained by performing classical MD simulations in the NPT ensemble for 1 ns, at the experimental density. Two systems have been studied: (i) a water box of 64 H_2O molecules, and (ii) an aqueous hydroxide in a water box of 63 H_2O, which corresponds to a hydroxide concentration of ~1 M. A background charge was used to neutralize the hydroxide charge. This method has been found to provide accurate results even for divalent ions.[68] The calculations were performed using the Car−Parrinello MD simulations[69] with the CPMD code.[70] The CPMD equations are integrated using a velocity Verlet algorithm with a time step of 0.19 fs and using a ficticious mass of 400 au for the electrons. The valence−core interaction was described by norm-conserving Troullier−Martins pseudopotentials.[71] A plane wave cutoff of 80 Ry was used. The electronic problem was solved using DFT with the BLYP exchange−correlation functional.[22,23] Recently, this methodology was shown to describe accurately the total radial distribution function obtained in X-ray experiments.[30] The simulations were performed in the canonical or NVT ensemble at 298 K using a Nose−Hoover chain thermostat[61] with a frequency of 1200 cm^{-1}. Two 30 ps simulations were performed for each system (water and aqueous hydroxide). The first simulation was run at a density of 1.00, and the second simulation was run at a density of 1.04. The size of the periodic cubic box used was (12.44 × 12.44 × 12.44 $Å^3$) and (12.23 × 12.23 × 12.23 $Å^3$), respectively. Merz−Kollman charges[74] were computed for 200 sets of coordinates extracted from the AIMD trajectories (60 ps) and used to evaluate the magnitude of charge transfer from the hydroxide to its coordination shell. The charges were found to be insensitive to the box size. Wannier function centers[72,73] (WFCs) were computed for each set of coordinates and used to calculate the water dipole moments.

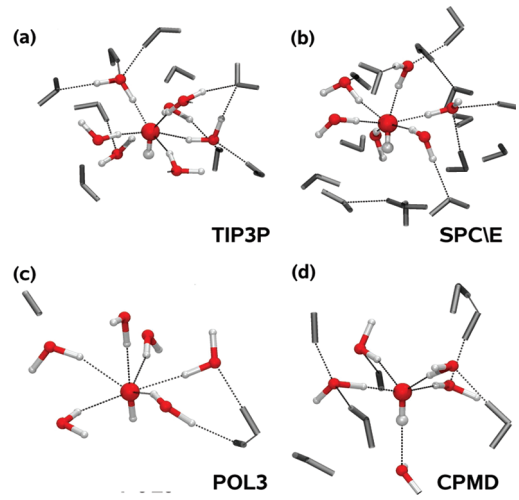

Figure 1. Coordination geometry around the hydroxide ion with different water models: (a) TIP3P, (b) SPC/E, (c) POL3, and (d) the reference AIMD calculations. Waters within 3.3 Å from the hydroxide oxygen O* are shown in CPK representation. An H-bond is counted if the distance between two heavy atoms (O* and O in this case) is less than 3.0 Å and the angle $O^*H^*O_w$ is larger than 120°.

Results

Comparison between Classical and AIMD Simulations. In Figure 1, we show representative snapshots from the classical and AIMD simulations. In the classical models the hydroxide ion is seen to be coordinated by six HB donors, while there are only four HB donors in AIMD. This qualitative picture of overcoordination in classical models is quantified in Figure 2, where we compare the RDF's and the coordination numbers obtained from the four models depicted in Figure 1 (the hydroxide atoms are denoted with a star, and water atoms are denoted with a subscript w). The three panels show the RDF's and the coordination numbers for O^*-O_w (top) O^*-H_w (middle), and H^*-O_w (bottom). The positions of the peaks in the RDF's are different in the classical MD and AIMD simulations. In particular, shorter O^*-O_w distances are observed with nonpolarizable waters (~2.6 Å), compared to (~2.8 Å) for AIMD simulations. The coordination numbers are also quite different in the two cases. As shown in the middle panel, there are approximately six HB donors in the classical MD simulations with nonpolarizable force fields but only approximately four HB donors in AIMD. Inclusion of polarization improves the classical results, but there are still sizable discrepancies especially in the H_w coordination (middle panel). Coordination of the

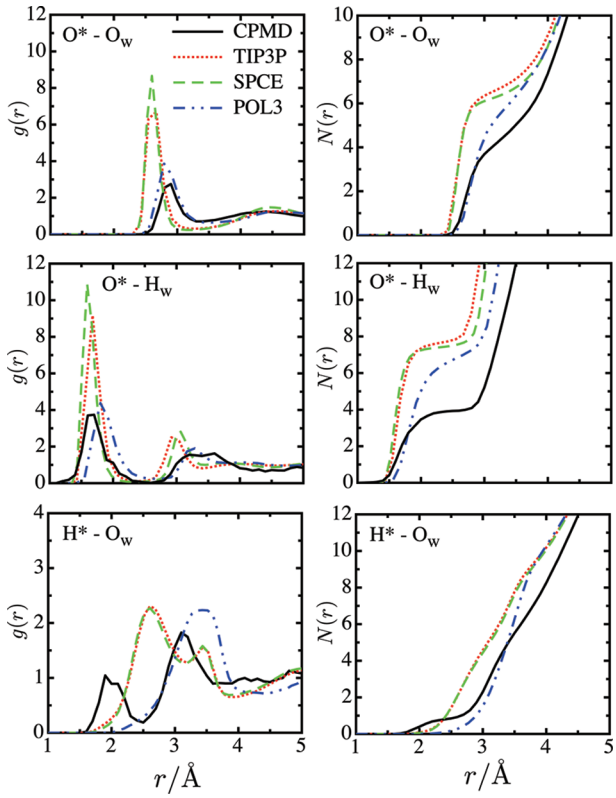

Figure 2. O*−O_w and O*−H_w partial RDF's (left) and running coordination numbers obtained by integration of the partial RDF's (right).

hydroxide hydrogen (H*) is also different in the classical and ab initio models (bottom panel). H* is coordinated by a water molecule during most of the simulation time in AIMD. Using a distance cutoff of 3.3 Å, corresponding to the minimum in the O*−O_w RDF, this bond is present >60% of the simulation time. The HB made by H* is longer compared to other HB's in the first shell, and the water exchange happens more rapidly, which points to a relatively weaker HB. In contrast, in the classical MD simulations there are no HB acceptors in the first solvation shell, and the hydroxide is coordinated only through HB donors. The differences between the classical and ab initio models with regard to the coordination numbers and the nature of HB's (i.e., donor or acceptor) indicate that the present classical models of hydroxide are not very realistic and need to be improved before use in dynamical calculations.

Coordination Geometry and Proton Transfer. The coordination geometry of aqueous hydroxide has been described previously.[16] Three dominant complexes are observed in AIMD: $OH^-(H_2O)_3$, $OH^-(H_2O)_4$, and $OH^-(H_2O)_5$. The distribution among these complexes is dependent upon the concentration and the counterion used in the simulation system.[16,19,20] We introduce the notation (X + Y) to describe the complexes, where X refers to HB donors that interact with the hydroxide O*, and Y refers to HB acceptors that interact with the hydroxide H*. In total, six common complexes can be identified: (3 + 1), (4 + 1), (5 + 1), (3 + 0), (4 + 0), and (5 + 0). The probability of occurrence of these complexes is shown in Figure 3 (top). The dominance of the (4 + Y) complex is clearly seen in this graph.

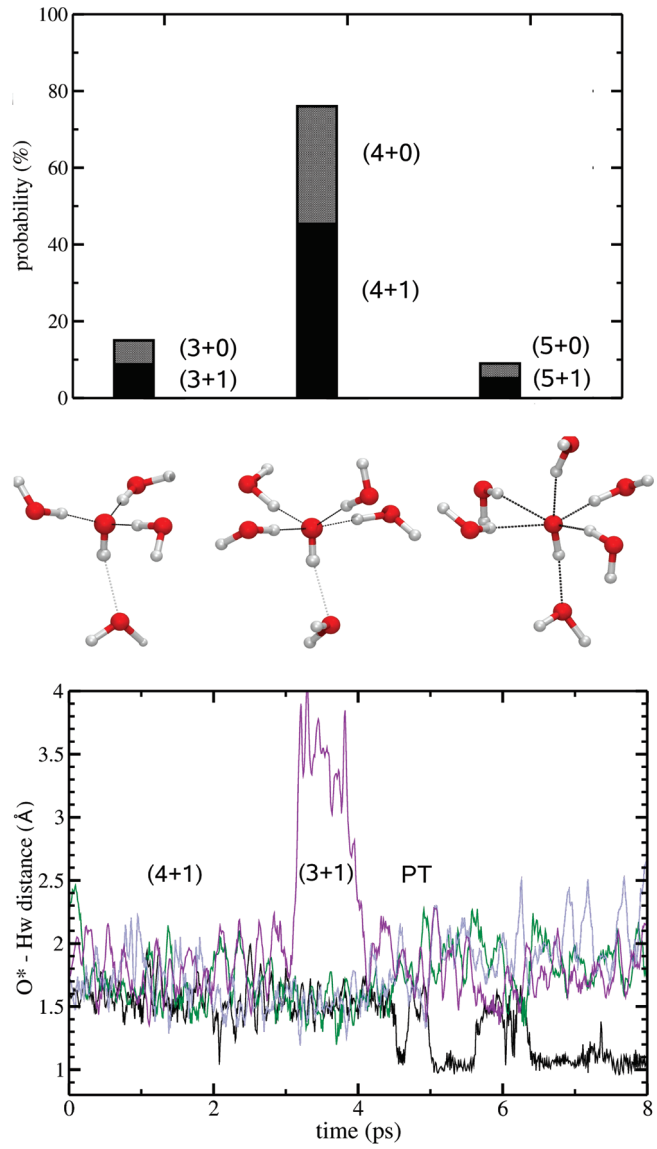

Figure 3. Histogram of the different coordination numbers in the first hydration shell obtained in the AIMD simulations (top). The probability that a water coordinates the hydroxide through the H* is shown in black. The middle panel shows typical snapshots for the most common complexes, (3 + 1), (4 + 1) and (5 + 1). The distance between the water ligands H_w and the hydroxide O* as a function of time in one of the simulations (bottom).

In Figure 3 (bottom), we also show the time series for the O*−H_w distance in one of the AIMD simulations. At the start of this simulation, the hydroxide forms a stable (4 + 1) complex. After ∼3 ps, one of the HB donating waters leaves the first coordination shell, and the hydroxide forms a (3 + 1) complex. From the O*−H_w distance, this water appears to come back to the solvation shell at ∼4 ps but, in fact, it does not form an HB with O*, hence the hydroxide remains in the (3 + 1) complex. In the (3 + 1) complex, the O*−H_w bonds become shorter, i.e., 1.53 ± 0.12 versus 1.70 ± 0.19 Å in the (4 + 1) complex. The smaller amplitudes in the O*−H_w vibrations indicate that the waters are also more tightly bound in the (3 + 1) complex. After about 4 ps, a proton transfer (PT) event is observed to occur in this simulation. In all the AIMD simulations performed, a PT

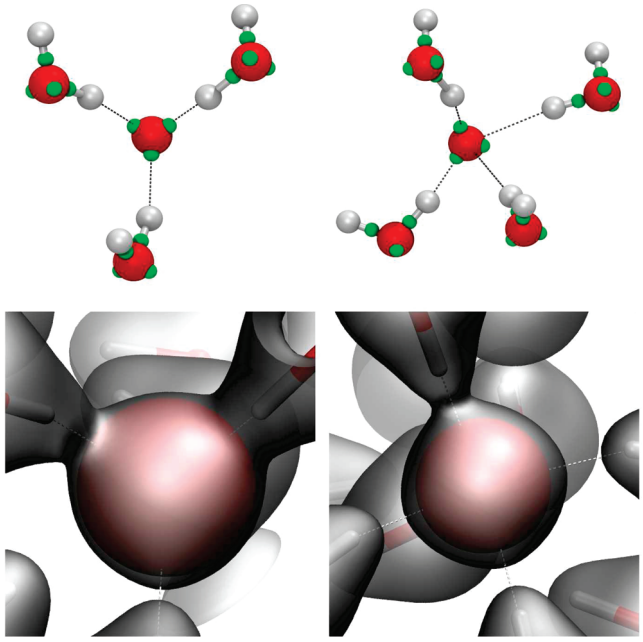

Figure 4. WFCs (top) and density isosurface of 0.05e (bottom) for the two most populated complexes in the simulations: (3 + 1) on the left and (4 + 1) on the right. The hydroxide is at the center of the images.

event has occurred within <5 ps of simulation in each case. The (3 + 1) complex has been identified as the main precursor to PT events in previous AIMD studies.[16] This is also observed in our simulations, which is consistent with the presolvation concept.[16,26] According to this concept, PT is more likely to occur in the (3 + 1) complex because the hydroxide will be transformed into a water that is already coordinated by four ligands in a tetrahedral geometry. The presence of frequent PT events has been used to rationalize the large diffusion coefficient of hydroxide relative to water.[26,27]

An important new result of the present simulations is the finding that the O*−H_w bonds are ∼0.2 Å shorter in the (3 + 1) complex compared to that of the (4 + 1) and that the amplitudes in the bond vibrations are reduced. In the next subsection, we also show that the electronic structure around the hydroxide O* is different in the (3 + 1) and (4 + 1) complexes, suggesting a new interpretation for the high reactivity of the (3 + 1) complex.

Electronic Structure. The electronic structure around the hydroxide ion has been previously investigated by Tuckerman et al.[16] Calculations of the electrostatic potential indicated a spherical distribution of the electron density around the hydroxide O*. Using a finer evaluation of the electron density around O*, here we find that the electron density deviates slightly from a perfect spherical distribution (Figure 4). In addition, the three Wannier function centers (WFCs), corresponding to the six valence electrons present in the electron cloud around O*, point directly toward the water ligands in the (3 + 1) complex but not in the (4 + 1) complex. In the (4 + 1) complex, the most common situation occurs when two WFCs point directly toward two water molecules, and the remaining one WFC is shared between two water molecules. Inspection of the trajectories reveals

Table 1. Comparison of the Dipole Moment of Waters in the First Hydration Shell of OH^- and Cl^- [a]

config.	dipole moment (D)	av. dist. (Å)
OH^- **3** + 1	3.52 (0.26)	2.52
OH^- **4** + 1	3.27 (0.42)	2.67
H_2O (bulk)	2.96 (0.30)	2.79
OH^- 4 + **1**	2.86 (0.23)	3.06
Cl^-	2.87 (0.27)	3.10

[a] The solvation configuration of the hydroxide complex is listed next to the ion. The nature of water used in the calculation (i.e., HB donor or acceptor) is indicated by boldface and underlining. The bulk water and Cl^- results are taken from refs 52 and 55. The last column gives the average distance of the hydration oxygen from the central ion or water.

that the waters directly interacting with a WFC are more likely to give a proton to the hydroxide, which indicates that they are forming the "most active" hydrogen bonds.[7,16]

To characterize the electronic structure further, we have calculated the average dipole moment of water molecules in the first solvation shell of hydroxide using the maximally localized Wannier functions (Table 1). Here we distinguish between different solvation complexes and whether the water is HB donor or acceptor. A general observation is that the dipole moment of the HB accepting water is lower than the bulk water value, while those of HB donors are much higher than the bulk water value. The dipole moment of the acceptor is seen to be very similar to those in the hydration shell of the Cl^- ion. As shown in the Table 1, there is a close correlation between the dipole moments of water molecules in the first solvation shell and their distance from the central ion or water. To some extent, this behavior can be traced to classical electrostatics where the polarization of water is proportional to the electric field and hence decreases with increasing distance from the ion. Charge transfer from the ion to the neighboring waters can also result in enhancement of the water dipoles, which is discussed further below.

Perhaps the most interesting result from the present AIMD simulations is that the average dipole moment of HB donors is 3.27 D in the (4 + 1) complex, which increases to 3.52 D in the (3 + 1) complex. To the best of our knowledge the water dipole moment in the (3 + 1) complex is the highest dipole moment reported for water in the hydration shell of monovalent or divalent ions. Furthermore, an analysis of the electrostatic potential indicates that the high water dipoles in the (3 + 1) complex cannot be simply explained by the lower dipole−dipole repulsion between first shell ligands, as in the case of other ions.[53] Instead, the observed differences in water polarization suggest that the (3 + 1) complex leads to slightly more covalent bonds that are stronger compared to the O*−H_w bonds in the (4 + 1) complex. The stronger bonds and the observed differences in the electronic structures between the two complexes are consistent with a PT mechanism that mainly involves the (3 + 1) complex, as observed in the AIMD simulations with the BLYP functional.

We have calculated the magnitude of the charge-transfer effects by computing the Merz−Kollman charges from the AIMD simulations.[74] For hydroxide in the gas phase, the charge on the O atom is −1.22*e* and on the H atom is +0.22*e*. In the aqueous phase, on the other hand, the charges

on the O and H atoms become, respectively, $-1.16e$ and $+0.32e$ for the $(4 + X)$ state and $-1.01e$ and $+0.29e$ for the $(3 + X)$ state. Thus the total charge on the hydroxide is increased from $-e$ in the gas phase to $-0.84e$ for the $(4 + X)$ state and $-0.72e$ for the $(3 + X)$ state. The corresponding charge transfers to the neighboring waters are $-0.16e$ and $-0.28e$, respectively, which are quite substantial and partly explain the increased dipole moments of waters in the hydration shell of hydroxide. Therefore, in addition to the proton transfer and induced polarization effects, the charge transfer provides another interesting phenomenon that is not described by classical models.

Fluctuations of Water Dipoles around the Hydroxide Ion. Whether the hydroxide ion is attracted to the air−water interface is a topical question. Suppression of the fluctuations of water dipoles around hydroxide has been proposed as a mechanism for its surface affinity.[37] Experimentally, sodium hydroxide is known to have one of the highest dielectric decrements for monovalent salts of monatomic ions. Buchner et al.[78] report that the dielectric decrement for sodium hydroxide is 20.9 ± 0.8 M^{-1} and that for sodium chloride is 15.2 ± 0.3 M^{-1}. Although the suppression of fluctuations by the hydroxide is consistent with what we know from its unusual solvation structure, the quantification of the high dielectric decrement related to this structure from computer simulations is challenging. In principle, this question can be answered most directly by calculating the ensemble averages for the total dipole moment and its fluctuations in a sphere centered around a hydroxide ion. However, classical studies aimed at computing this property suggest that simulations in the order of 1−2 ns are required to reach convergence.[75,76] Our attempt to estimate the dielectric decrement from an AIMD simulation lasting ∼60 ps did not succeed because the present sampling time was not sufficient to obtain a statistically meaningful average that could be compared with experiments. Similarly, we note that a recent study[77] of statistical uncertainties in determination of the diffusion coefficient from AIMD simulations has concluded that ∼500 ps would be required in ambient conditions, which is an order of magnitude longer than that used here.

In order to obtain a semiquantitative description of the reduction of dipole fluctuations, we have computed the relaxation time, τ, for the orientational autocorrelation function, $C(t)$, of O−H vectors in the simulation box. The computed orientational relaxation for waters around the hydroxide ion and for bulk water are shown in Figure 5. In the case of hydroxide, the relaxation time is found to be an order of magnitude larger than that of bulk water, which shows that the presence of hydroxide has a substantial stabilizing effect on the neighboring waters. A more intuitive picture emerges from the inspection of the trajectories in the two simulation systems. A hydroxide ion is observed to rotate slower compared to a central water molecule in the bulk system. Furthermore, the hydration waters around the hydroxide ion undergo mainly translational motion and exhibit little rotation. In contrast, the orientations of the waters around the central water change considerably during the same period. This provides a qualitative illustration of how the presence of a hydroxide ion has a stabilizing effect on the neighboring water molecules and thus suppresses the dipole fluctuations in the hydroxide system relative to bulk water. These results are consistent with experimental dielectric decrements for hydroxide.[78] We are currently exploring the consequences of this effect in more detail.

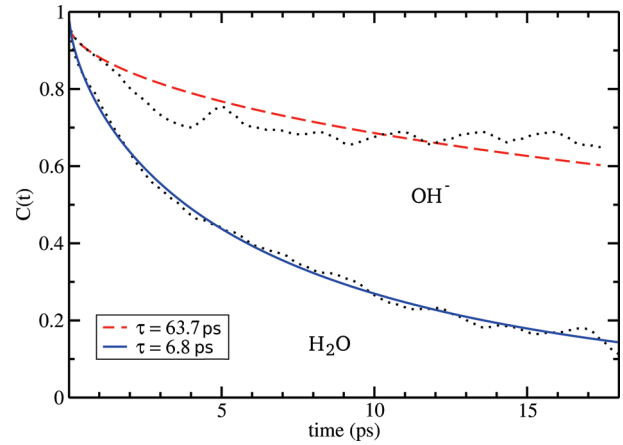

Figure 5. Comparison of the orientational correlation time (τ) of waters around a hydroxide ion (dashed line) with that of a central water in bulk (solid line). The lines are obtained by fitting, $C(t) = e^{-t/\tau}$, to the AIMD results (indicated with dots), which are calculated from 30 ps AIMD simulations. The correlation times for the two cases are given in the box.

Conclusions

The comparison between the classical and ab initio molecular dynamics (AIMD) simulations of aqueous hydroxide in this work indicates that the structural and electronic properties of aqueous hydroxide are not well described by current point charge models. In this regard, the newly proposed charged ring model[79] offers a considerable improvement as it predicts the four hydrogen-bond (HB) donor waters as the dominant configuration. However, one shortcoming of this model is that it fails to reproduce the weakly bound HB acceptor. Further improvement is possible, for example, by constructing a classical model that can account for the proton transfer events observed in the AIMD simulations, see, e.g., refs 80 and 81.

We have observed several proton transfer events during the AIMD simulations. In each case, proton transfer occurred not in the dominant $(4 + 1)$ complex but in the rarer $(3 + 1)$ complex. This is consistent with the presolvation concept, that is, proton transfer is more likely to occur when the hydroxide ion turns into a water molecule with a tetrahedral coordination. Calculation of the dipole moments of hydration waters has shed further light on the unique structure of the hydroxide complex. Already in the $(4 + 1)$ complex, the average dipole moment of hydration waters is substantially larger than that of bulk water, which is opposite to what happens for monovalent ions. In the case of the $(3 + 1)$ complex, the dipole moment attains a much larger value, exceeding even those in the hydration shell of a divalent ion. These unique properties make the aqueous hydroxide an ideal system for testing the polarizable force fields currently under construction.

We have also discussed how fluctuations of water dipoles around the hydroxide ion are reduced when compared to bulk

water due to the extra stability provided by the hydroxide. This effect may help to explain the affinity of hydroxide ions near the water surface and needs to be studied further with improved sampling.

Acknowledgment. This work was supported by grants from the Australian Research Council. Calculations were performed using the SGI Altix clusters at the National Computational Infrastructure (Canberra), the Australian Center for Advanced Computing and Communications (Sydney), and the Victorian Partnership for Advanced Computing (Melbourne).

References

(1) Atkins, P.; de Paula, J. *Atkins' Physical Chemistry*; 7th ed.; Oxford University Press: Oxford, U.K., 2002; pp 766.

(2) Tuckerman, M. E.; Laasonen, K.; Sprik, M.; Parrinello, M. *J. Chem. Phys.* **1995**, *103*, 150–161.

(3) Tuckerman, M. E.; Marx, D.; Klein, M. L.; Parrinello, M. *Science* **1997**, *275*, 817–820.

(4) Marx, D.; Tuckerman, M. E.; Hutter, J.; Parrinello, M. *Nature* **1999**, *397*, 601–604.

(5) Marx, D. *ChemPhysChem* **2006**, *7*, 1848–1870.

(6) Asthagiri, D.; Pratt, L. R.; Kress, J. D. *Proc. Natl. Acad. Sci. U.S.A.* **2005**, *102*, 6704–6708.

(7) Marx, D.; Chandra, A.; Tuckerman, M. E. *Chem. Rev.* **2010**, *110*, 2174–2216.

(8) Agmon, N. *Chem. Phys. Lett.* **1995**, *244*, 456–462.

(9) Lobaugh, J.; Voth, G. A. *J. Chem. Phys.* **1996**, *104*, 2056–2069.

(10) Schmitt, U. W.; Voth, G. A. *J. Chem. Phys.* **1999**, *111*, 9361–9381.

(11) Voth, G. A. *Acc. Chem. Res.* **2006**, *39*, 143–150.

(12) Ando, K.; Hynes, J. T. *J. Phys. Chem. B* **1997**, *101*, 10464–10478.

(13) Vuilleumier, R.; Borgis, D. *J. Chem. Phys.* **1999**, *111*, 4251–4266.

(14) Kornyshev, A. A.; Kuznetsov, A. M.; Spohr, E. J.; Ulstrup, J. *J. Phys. Chem. B* **2003**, *107*, 3351–3366.

(15) Brancato, G.; Tuckerman, M. E. *J. Chem. Phys.* **2005**, *122*, 224507.

(16) Tuckerman, M. E.; Marx, D.; Parrinello, M. *Nature* **2002**, *417*, 925–929.

(17) Huckel, E. *Z. Elektrochem.* **1928**, *34*, 546–562.

(18) Agmon, N. *Chem. Phys. Lett.* **2000**, *319*, 247–252.

(19) Zhu, Z.; Tuckerman, M. E. *J. Chem. Phys. B* **2002**, *106*, 8009–8018.

(20) Chen, B.; Ivanov, I.; Park, J. M.; Parrinello, M.; Klein, M. L. *J. Phys. Chem. B* **2002**, *106*, 12006–12016.

(21) Perdew, J. P.; Wang, Y. *Phys. Rev. B: Condens. Matter Mater. Phys.* **1992**, *45*, 13244–13249.

(22) Becke, A. D. *Phys. Rev. A: At., Mol., Opt. Phys.* **1988**, *38*, 3098–3100.

(23) Lee, C. T.; Yang, W. T.; Parr, R. G. *Phys. Rev. B: Condens. Matter Mater. Phys.* **1988**, *37*, 785–789.

(24) Asthagiri, D.; Pratt, L. R.; Kress, J. D.; Gomez, M. A. *Proc. Natl. Acad. Sci. U.S.A.* **2004**, *101*, 7229–7233.

(25) Hamprecht, F. A.; Cohen, A. J.; Tozer, D. J.; Handy, N. C. *J. Chem. Phys.* **1998**, *109*, 6264–6271.

(26) Tuckerman, M. E.; Chandra, A.; Marx, D. *Acc. Chem. Res.* **2006**, *39*, 151–158.

(27) Chandra, A.; Tuckerman, M. E.; Marx, D. *Phys. Rev. Lett.* **2007**, *99*, 145901.

(28) Imberti, S.; Botti, A.; Bruni, F.; Cappa, G.; Ricci, M. A.; Soper, A. K. *J. Chem. Phys.* **2005**, *122*, 194509.

(29) McLain, S. E.; Imberti, S.; Soper, A. K.; Botti, A.; Bruni, F.; Ricci, M. A. *Phys. Rev. B: Condens. Matter Mater. Phys.* **2006**, *74*, 094201.

(30) Megyes, T.; Balint, S.; Grosz, T.; Radnai, T.; Bako, I.; Sipos, P. *J. Chem. Phys.* **2008**, *128*, 044501.

(31) Marinova, K. G.; Alargova, R. G.; Denkov, N. D.; Velev, O. D.; Petsev, D. N.; Ivanov, I. B.; Borwankar, R. P. *Langmuir* **1996**, *12*, 2045–2051.

(32) Beattie, J. K.; Djerdjev, A. M. *Angew. Chem., Int. Ed.* **2004**, *43*, 3568–3571.

(33) Petersen, P. B.; Saykally, R. J. *J. Phys. Chem. B* **2005**, *109*, 7976–7980.

(34) Petersen, P. B.; Saykally, R. J. *Chem. Phys. Lett.* **2008**, *458*, 255–261.

(35) Tian, C. S.; Shen, Y. R. *Proc. Natl. Acad. Sci. U.S.A.* **2009**, *106*, 15148–15153.

(36) Creux, P.; Lachaise, J.; Graciaa, A.; Beattie, J. K.; Djerdjev, A. M. *J. Phys. Chem. B* **2009**, *113*, 14146–14150.

(37) Gray-Weale, A.; Beattie, J. K. *Phys. Chem. Chem. Phys.* **2009**, *11*, 10994–11005.

(38) Orr, J. C.; Fabry, V. J.; Aumont, O.; Bopp, L.; Doney, S. C.; Feely, R. A.; Gnanadesikan, A.; Gruber, N.; Ishida, A.; Joos, F.; et al. *Nature* **2005**, *437*, 681–686.

(39) Mucha, M.; Frigato, T.; Levering, L. M.; Allen, H. C.; Tobias, D. J.; Dang, L. X.; Jungwirth, P. *J. Phys. Chem. B* **2005**, *109*, 7617–7623.

(40) Buch, V.; Milet, A.; Vacha, R.; Jungwirth, P.; Devlin, J. P. *Proc. Natl. Acad. Sci. U.S.A.* **2007**, *104*, 7342–7347.

(41) Wick, C. D.; Kuo, I. F. W.; Mundy, C. J.; Dang, L. X. *J. Chem. Theory Comp.* **2007**, *3*, 2002–2010.

(42) Petersen, M. K.; Iyengar, S. S.; Day, T. J. F.; Voth, G. A. *J. Phys. Chem. B* **2004**, *108*, 14804–14806.

(43) Iuchi, S.; Chen, H.; Paesani, F.; Voth, G. A. *J. Phys. Chem. B* **2009**, *113*, 4017–4030.

(44) Kudin, K. N.; Car, R. *J. Am. Chem. Soc.* **2008**, *130*, 3915–3919.

(45) Mundy, C. J.; Kuo, I. F. W.; Tuckerman, M. E.; Lee, H. S.; Tobias, D. J. *Chem. Phys. Lett.* **2009**, *481*, 2–8.

(46) Lee, H. S.; Tuckerman, M. E. *J. Phys. Chem. B* **2009**, *113*, 2144–2151.

(47) Wick, C. D.; Dang, L. X. *J. Phys. Chem. B* **2009**, *113*, 6356–6364.

(48) Bako, I.; Hutter, J.; Palinkas, G. *J. Chem. Phys.* **2002**, *117*, 9838–9843.

(49) Krekeler, C.; Hess, B.; Delle Site, L. *J. Chem. Phys.* **2006**, *125*, 054305.

(50) Krekeler, C.; Delle Site, L. *J. Phys.: Condens. Matter* **2007**, *19*, 192101.

(51) Whitfield, T. W.; Varma, S.; Harder, E.; Lamoureux, G.; Rempe, S. B.; Roux, B. *J. Chem. Theory Comput.* **2007**, *3*, 2068–2082.

(52) Ikeda, T.; Boero, M.; Terakura, K. *J. Chem. Phys.* **2007**, *126*, 034501.

(53) Bucher, D.; Kuyucak, S. *J. Phys. Chem. B* **2008**, *112*, 10786–10790.

(54) Scipioni, R.; Schmidt, D. A.; Boero, M. *J. Chem. Phys.* **2009**, *130*, 024502.

(55) Guardia, E.; Skarmoutsos, I.; Masia, M. *J. Chem. Theory Comp.* **2009**, *5*, 1449–1453.

(56) Jorgensen, W. L.; Chandrasekhar, J.; Madura, J. D.; Impey, R. W.; Klein, M. L. *J. Chem. Phys.* **1983**, *79*, 926–935.

(57) Berendsen, H. J. C.; Grigera, J. R.; Straatsma, T. P. *J. Phys. Chem.* **1987**, *91*, 6269–6271.

(58) Vacha, R.; Horinek, D.; Berkowitz, M. L.; Jungwirth, P. *Phys. Chem. Chem. Phys.* **2008**, *10*, 4975–4980.

(59) Nose, S. *J. Chem. Phys.* **1984**, *81*, 511–519.

(60) Hoover, W. G. *Phys. Rev. A: At., Mol., Opt. Phys.* **1985**, *31*, 1695–1697.

(61) Martyna, G. J.; Klein, M. L.; Tuckerman, M. *J. Chem. Phys.* **1992**, *97*, 2635–2643.

(62) Phillips, J. C.; Braun, R.; Wang, W.; Gumbart, J.; Tajkhorshid, E.; Villa, E.; Chipot, C.; Skeel, R. D.; Kale, L.; Schulten, K. *J. Comput. Chem.* **2005**, *26*, 1781–1802.

(63) Darden, T.; York, D.; Pedersen, L. *J. Chem. Phys.* **1993**, *98*, 10089–10092.

(64) Gray-Weale, A. *Program toyMD*; Monash University: Victoria, Australia, 2010; https://confluence-vre.its.monash.edu.au/display/toyMD/.

(65) Caldwell, J. W.; Kollman, P. A. *J. Phys. Chem.* **1995**, *99*, 6208–6219.

(66) Ryckaert, J.-P.; Ciccotti, G.; Berendsen, H. J. C. *J. Comput. Phys.* **1977**, *23*, 327–341.

(67) Hockney, R. W.; Eastwood, J. W. *Computer Simulation Using Particles*; Institute of Physics: Bristol, U.K., 1981.

(68) Todorova, T.; Hunenberger, P. H.; Hutter, J. *J. Chem. Theory Comput.* **2008**, *4*, 779–789.

(69) Car, R.; Parrinello, M. *Phys. Rev. Lett.* **1985**, *55*, 2471–2474.

(70) Hutter, J.; Alavi, A.; Deutch, T.; Bernasconi, M.; Goedecker, S.; Marx, D.; Tuckerman, M.; Parrinello, M. *Technical Report*; MPI fur Festkorperforschung and IBM Zurich Research Laboratory: Zurich, Switzerland, 1995−1999.

(71) Troullier, N.; Martins, J. L. *Phys. Rev. B: Condens. Matter Mater. Phys.* **1991**, *43*, 1993–2006.

(72) Marzari, N.; Vanderbilt, D. *Phys. Rev. B: Condens. Matter Mater. Phys.* **1997**, *56*, 12847–12865.

(73) Silvestrelli, P. L.; Parrinello, M. *J. Chem. Phys.* **1999**, *111*, 3572–3580.

(74) Singh, U. C.; Kollman, P. A. *J. Comput. Chem.* **1984**, *5*, 129–145.

(75) Ronne, C.; Thrane, L.; Astrand, P. O.; Wallqvist, A.; Mikkelsen, K. V.; Keiding, S. R. *J. Chem. Phys.* **1997**, *107*, 5319–5331.

(76) Heinz, T. N.; van Gunsteren, W. F.; Hunenberger, P. H. *J. Chem. Phys.* **2001**, *115*, 1125–1136.

(77) Kuo, I. F. W.; Mundy, C. J.; McGrath, M. J.; Siepman, J. I. *J. Chem. Theory Comp.* **2006**, *2*, 1274–1281.

(78) Buchner, R.; Hefter, G.; May, P. M.; Sipos, P. *J. Phys. Chem. B* **1999**, *103*, 11186–11190.

(79) Ufimtsev, I. S.; Kalinichev, A. G.; Martinez, T. J.; Kirkpatrick, R. J. *Chem. Phys. Lett.* **2007**, *442*, 128–133.

(80) Billeter, S. R.; van Gunsteren, W. F. *J. Phys. Chem. A* **1998**, *102*, 4669–4678.

(81) Pomes, R.; Roux, B. *Biophys. J.* **2002**, *82*, 2304–2316.

CT1003719